Soft Materials

Deutsche Ausgabe: DOI: 10.1002/ange.201606895
Internationale Ausgabe: DOI: 10.1002/anie.201606895

Frequency-Driven Self-Organized Helical Superstructures Loaded with Mesogen-Grafted Silica Nanoparticles

*Karla G. Gutierrez-Cuevas[+], Ling Wang[+], Zhi-gang Zheng, Hari K. Bisoyi, Guoqiang Li, Loon-Seng Tan, Richard A. Vaia, and Quan Li**

Abstract: *Adding colloidal nanoparticles into liquid-crystal media has become a promising pathway either to enhance or to introduce novel properties for improved device performance. Here we designed and synthesized new colloidal hybrid silica nanoparticles passivated with a mesogenic monolayer on the surface to facilitate their organo-solubility and compatibility in a liquid-crystal host. The resulting nanoparticles were identified by ^1H NMR spectroscopy, TEM, TGA, and UV/Vis techniques, and the hybrid nanoparticles were doped into a dual-frequency cholesteric liquid-crystal host to appraise both their compatibility with the host and the effect of the doping concentration on their electro-optical properties. Interestingly, the silica-nanoparticle-doped liquid-crystalline nanocomposites were found to be able to dynamically self-organize into a helical configuration and exhibit multi-stability, that is, homeotropic (transparent), focal conic (opaque), and planar states (partially transparent), depending on the frequency applied at sustained low voltage. Significantly, a higher contrast ratio between the transparent state and scattering state was accomplished in the nanoparticle-embedded liquid-crystal systems.*

Cholesteric liquid crystals (LCs) with a self-organized helical disposition of molecules not only exhibit fascinating scientific phenomena but also have found practical applications in devices such as temperature sensors, reflective displays, color filters, mirrorless lasers, and light shutters.[1] Recently, cholesteric LCs fabricated from nematic dual frequency LCs (DFLCs) with frequency dependence of the dielectric anisotropy have attracted considerable attention because both focal conic and planar configuration of such dual frequency cholesteric LCs (DFCLCs) can be switched depending on the frequency of the applied voltage, developing cholesteric reflective displays, fast switching bistable light shutters, and bistable intensity modulators.[2] On the other hand, embedded metallic, semiconducting, and carbon nanomaterials have recently been employed to modify the properties of LCs.[3] Dielectric silica (SiO_2) nanoparticles are the early examples of nanoparticle dispersions into LC matrices.[4] An advantage of SiO_2 nanoparticles in LCs is the modulation of the refractive index of LC media, which could be exploited to develop hybrid liquid-crystalline nanocomposites with improved properties.[5] Though commercially available SiO_2 nanoparticles were able to modify some properties of LCs, their dispersions were not stable and only very small amount of the particles can be dispersed because of their strong propensity to aggregate or poor compatibility in LC matrix.[6] To circumvent this difficulty, surface functionalization of SiO_2 nanoparticles has been adopted which led to some interesting results.[7] Nevertheless, their functionalization with mesogenic or pro-mesogenic moieties is still a challenging task from the synthetic point of view, albeit this strategy could enable good dispersion and compatibility in LC media.[8] Here we functionalized SiO_2 nanoparticles with a covalently attached mesogenic monolayer through silane coupling agents and investigated their effect on the electro-optical property of a DFCLC system. The resulting hybrid nanoparticles (M-SiO_2) were organo-soluble without noticeable aggregation and were able to disperse well in the DFCLC host with the concentration as high as 3.0 wt%. Interestingly, M-SiO_2 nanoparticles enabled to greatly enhance the electro-optical properties compared to the pure DFCLC. The light transmittance of the M-SiO_2 embedded LC nanocomposite films can be easily tuned by simply modulating the frequency of an applied constant voltage. Moreover, the M-SiO_2-doped system exhibited a higher contrast ratio compared with the pure DFCLC. To the best of our knowledge, this is for the first time that the effect of mesogen-grafted SiO_2 nanoparticles embedded in a dual-frequency LC matrix is explored.

The synthesis of M-SiO_2 nanoparticles is straightforward in a facile manner as depicted in Scheme 1. The commercially available SiO_2-OH nanoparticles were reacted with (3-amino propyl)-triethoxy silane (APTES) in ethanol to afford the intermediate SiO_2-NH_2 nanoparticles followed by coupling with mesogenic 4-octyl-4-biphenylcarboxylic acid through the amide bond linkage. The resulting M-SiO_2 nanoparticles were characterized by proton nuclear magnetic resonance (^1H NMR) spectroscopy, thermogravimetric analysis (TGA), transmission electron microscopy (TEM), energy-dispersive X-ray (EDX) spectroscopy, and UV/Vis analysis. The M-SiO_2

[*] K. G. Gutierrez-Cuevas,[+] Dr. L. Wang,[+] Dr. Z.-g. Zheng, Dr. H. K. Bisoyi, Prof. Q. Li
Liquid Crystal Institute and
Chemical Physics Interdisciplinary Program, Kent State University
Kent, OH 44242 (USA)
E-mail: qli1@kent.edu
Prof. G. Li
Department of Ophthalmology and Visual Science and
Department of Electrical and Computer Engineering
Ohio State University
Columbus, OH 43212 (USA)
Dr. L.-S. Tan, Dr. R. A. Vaia
Materials and Manufacturing Directorate
Air Force Research Laboratory
Wright-Patterson AFB, OH 45433 (USA)
[+] These authors contributed equally to this work.

Supporting information for this article can be found under: http://dx.doi.org/10.1002/anie.201606895.

 © 2016 Wiley-VCH Verlag GmbH & Co. KGaA, Weinheim

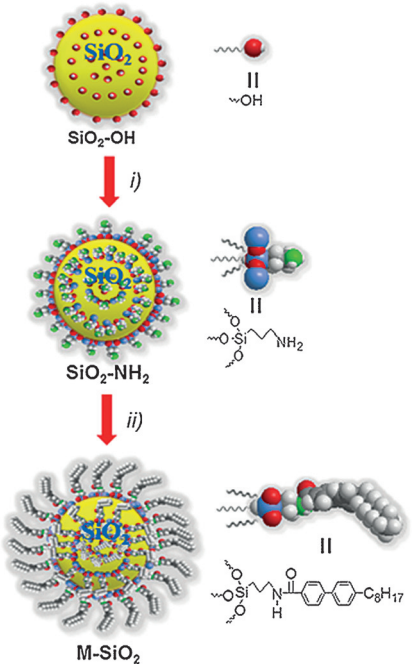

Scheme 1. Synthesis of mesogen-grafted silica nanoparticles (M-SiO_2). i) (3-amino propyl)-triethoxy silane, ethanol, and ii) 4-octyl-4-biphenyl-carboxylic acid, *N*-(3-dimethylaminopropyl)-*N*-ethylcarbodiimide hydrochloride, THF.

nanoparticles were able to disperse well in organic solvents such as THF and $CHCl_3$ even after being stored for several weeks at room temperature. The ^{1}H NMR spectrum of M-SiO_2 nanoparticles displayed the presence of aromatic signals at lower fields, with a chemical shift around 7.5 ppm associated with the protons of the aromatic groups of the covalently attached mesogen (see Figure S1 in the Supporting Information), whereas these signals were not present in the spectrum of SiO_2-NH_2 nanoparticles.[9] From the TGA analysis (Figure S2), the SiO_2-OH nanoparticles had a total loss of 1.78 wt%, which is associated with the presence of silanol groups on their surface. The TGA curve of the SiO_2-NH_2 nanoparticles presents one decomposition step at about 410 °C related to the chemical attachment of APTES molecules onto the surface. The total weight loss was 6.65 wt%, indicating that 4.8 wt% of APTES was attached to the SiO_2 nanoparticle surface. In contrast, the TGA plot of the M-SiO_2 nanoparticles displays a two-step degradation curve, indicating progressive decomposition of surface groups, one due to the mesogens at 220 °C and the other due to the APTES groups at 410 °C; and the total loss was 9.74 wt%.

The M-SiO_2 nanoparticles exhibited fluorescence at certain UV range, which could be used as a simple technique to monitor the presence of the SiO_2 nanoparticles in solution, as demonstrated in Figure 1a. The SiO_2-OH nanoparticles were water soluble whereas the M-SiO_2 nanoparticles were soluble in organic solvents after surface modification. UV-induced fluorescence clearly demonstrates good dispersion of M-SiO_2 nanoparticles in the organic solvent. Transmission electron microscope (TEM) images (Figure 1b) also showed apparent well-dispersion of M-SiO_2 nanoparticles, demonstrating no noticeable aggregation in solution compared with the precursor SiO_2-OH and SiO_2-NH_2 nanoparticles. The serious overlap of SiO_2-OH nanoparticles was observed in the TEM grid due to the strong hydrogen bonding of the silanol groups. In contrast, when the mesogen was linked, no nanoparticle overlap was observed in the TEM image, which indicates the improvement of nanoparticle dispersion. The size of the M-SiO_2 nanoparticles was 26.97 ± 2.92 nm, calculated by TEM considering 500 nanoparticles. The size distribution is showed in Figure S4 (top). Additionally, the presence of the nitrogen, oxygen and silicon in the functionalized nanoparticles was observed from EDX spectrum (see Figure S4 (bottom) in the Supporting Information).

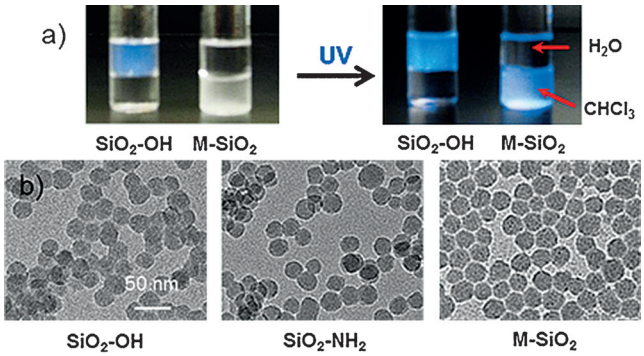

Figure 1. a) Photographs of SiO_2 nanoparticle solutions before (SiO_2-OH) and after ligand exchange (M-SiO_2) in a water-chloroform mixture with and without 365 nm UV irradiation, and b) TEM images of SiO_2-OH, SiO_2-NH_2, and M-SiO_2 nanoparticles.

To explore the effect of M-SiO_2 nanoparticles on the properties of the DFCLC host, 0.5, 1.0, 1.5, 2.0 and 3.0 wt% M-SiO_2 nanoparticles were, respectively doped into the DFCLC with a pitch length of around 1.6 μm. The DFCLC used here is comprised of a commercially available chiral dopant S811 (6 wt%) and 94 wt% nematic DFLC (DP002-016, $T_{N\text{-}I} = 104$ °C, $\Delta n = 0.268$). The M-SiO_2-doped DFCLC nanocomposites were capillary-filled into the LC cells assembled from untreated glass substrates with 15 μm cell gap. Their liquid-crystalline behavior at room temperature was observed under a polarized optical microscopy (POM) with crossed polarizers in transmission mode. At the initial state, all cells displayed typical oily streak cholesteric textures (Figure 2). No evident aggregates were observed in the POM textures of the nanocomposites, suggesting that the M-SiO_2 dispersed homogeneously in the DFCLC host even when the M-SiO_2 concentration was increased up to 3.0 wt% (Figure 2f). It was found that the cholesteric (N*)-isotropic (I) and I-N* phase transition decreased with the increase of nanoparticle concentration as shown in Supporting Information Figure S5. One possible explanation of these observations is related to the decreased ordering in the DFCLC matrix after doping the M-SiO_2 nanoparticles in the medium, as reported before for other nanocolloidal systems.[10]

The electro-optical properties of M-SiO_2/DFCLC nanocomposites were further investigated by applying an AC field at different frequencies and a constant voltage of 20 V. Figure 3 displays the POM textures of 2 wt% M-SiO_2 doped DFCLC and pure DFCLC host with different frequencies at

 © 2016 Wiley-VCH Verlag GmbH & Co. KGaA, Weinheim

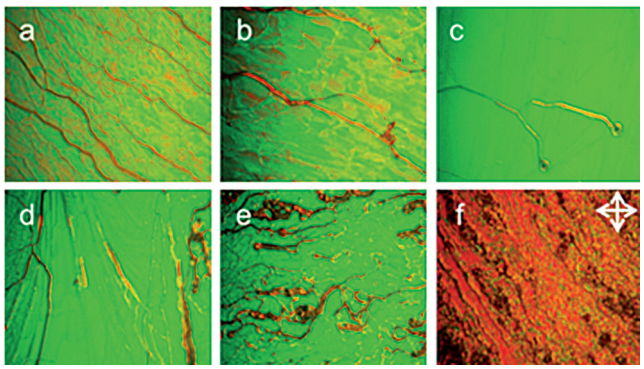

Figure 2. POM textures of DFCLC nanocomposites with different concentration of M-SiO_2 nanoparticles at 0 wt% (a), 0.5 wt% (b), 1.0 wt% (c), 1.5 wt% (d), 2.0 wt% (e), and 3.0 wt% (f) at room temperature.

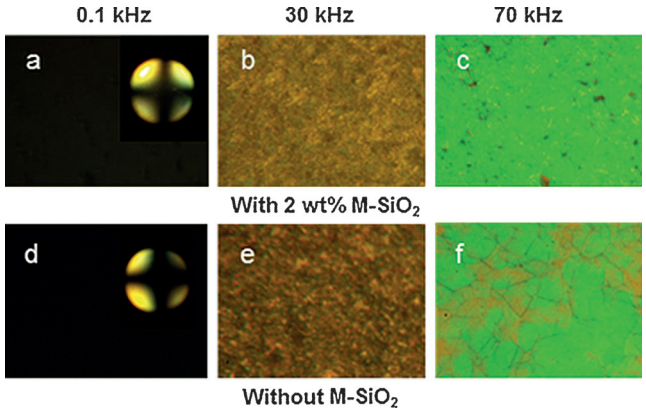

Figure 3. POM textures of DFCLC with 2 wt% M-SiO_2 and without M-SiO_2 at 0.1 kHz, 30 kHz, and 70 kHz under an applied constant voltage of 20 V.

a constant voltage. As it can be observed, at the low frequency of 0.1 kHz, a homeotropic alignment (Figure 3a and d) was formed, where the helix was unwound by a dielectric coupling between LC molecules and the vertical electric field. The inset shows the conoscopic interference pattern with a Maltese cross, confirming the existence of the molecular alignment perpendicular to the substrate, that is, homeotropic (H) state. Upon increasing the frequency to 30 kHz, a focal conic (FC) texture was developed (Figure 3b and e), and the light was scattered due to the random orientation of the helical axes of the DFCLC domains. When the frequency was further increased to 70 kHz, the LC arrangement transformed into a planar state where the helical axis is perpendicular to the substrates of the LC cell (Figure 3c and f). The transmittance and contrast ratio of DFCLC nanocomposites with different concentrations of M-SiO_2 nanoparticles were evaluated through the transmission spectra detected by a fiber-optic spectrometer. The higher and lower transmission intensities were defined as I^+ in the homeotropic state and I^- when the light source was extinguished; the contrast ratio (CR) was defined as $CR = T^+/T^-$ where T^+ was assigned to the transmission intensity in the homeotropic state and T^- was assigned to transmission of the FC or the planar state. As

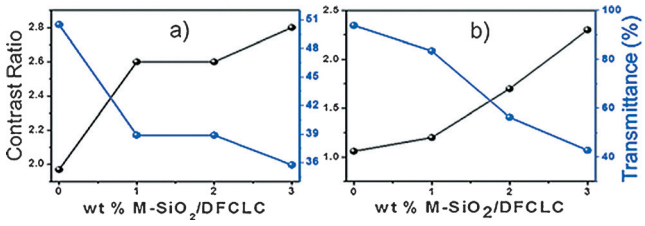

Figure 4. Contrast ratio (black) and transmittance (blue) curves of incident light (550 nm) with different concentrations of M-SiO_2 nanoparticles in DFCLC at a) focal conic state (30 kHz, 20 V) and b) planar state (70 kHz, 20 V).

shown in Figure 4a, an improved contrast ratio for all M-SiO_2-doped DFCLC nanocomposites compared with the pure DFCLC host was attained. Nevertheless, in the planar state (higher frequencies), the transmittance decreased with the increase of the M-SiO_2 content (Figure 4b), which yielded a partially transparent state.

Figure 5 shows the photographs of a colorful image behind the two LC cells, respectively, containing 2 wt% M-SiO_2 doped DFCLC (top) and the pure DFCLC host (bottom) in the H (transparent), FC (scattered) and planar states (partially transparent or transparent). The colorful image (yellow sphere, red helix and space-filling model of surfactants on black-doted blue background) behind both LC cells can be clearly observed at low frequency (Figure 5a and d, 0.1 kHz, H state), whereas when a higher frequency was applied (Figure 5b and e, 30 kHz, FC) the colorful image behind both cells was not visible due to light scattering of the FC domains. However, for the DFCLC thin film containing 2 wt% M-SiO_2, the scattering is greatly enhanced and the colorful image behind the cell cannot be perceived due to the stronger scattering effect from the embedded nanoparticle system. When a higher frequency was applied, both the pure DFCLC and M-SiO_2-doped DFCLC reconfigured into the planar state (Figure 5c and f, 70 kHz, planar state), however the M-SiO_2-doped sample was partially transparent due to the influence of silica nanoparticles in the helical arrangement in

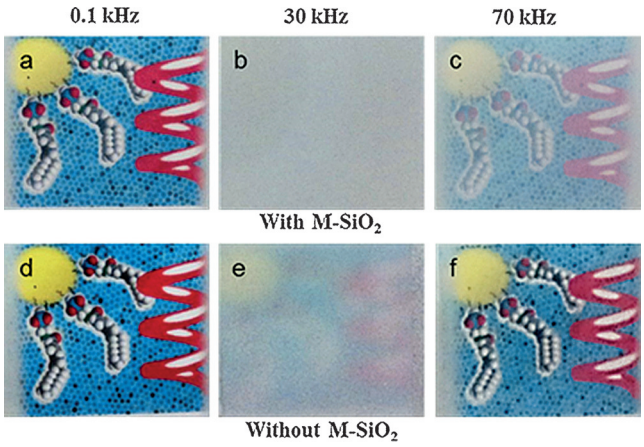

Figure 5. Photographs of a colorful image positioned behind the LC cells containing DFCLC with 2 wt% M-SiO_2 (a, b, c) and without M-SiO_2 (d, e, f) at 0.1 kHz, 30 kHz and 70 kHz, respectively under an applied constant bias of 20 V.

© 2016 Wiley-VCH Verlag GmbH & Co. KGaA, Weinheim

the LC cell. It is noteworthy that both P and FC states were found to be stable for a long time even when the applied field was removed, since no noticeable change in the states, that is, partially transparent and opaque, was observed (Figures S8 and S9).

To have a clear insight about the possible arrangement of LC molecules in the M-SiO_2 doped DFCLC and the pure DFCLC, a schematic representation of the M-SiO_2 doped DFCLC nanocomposite and pure DFCLC is illustrated in Figure 6. At lower frequencies, the helix is unwound and the

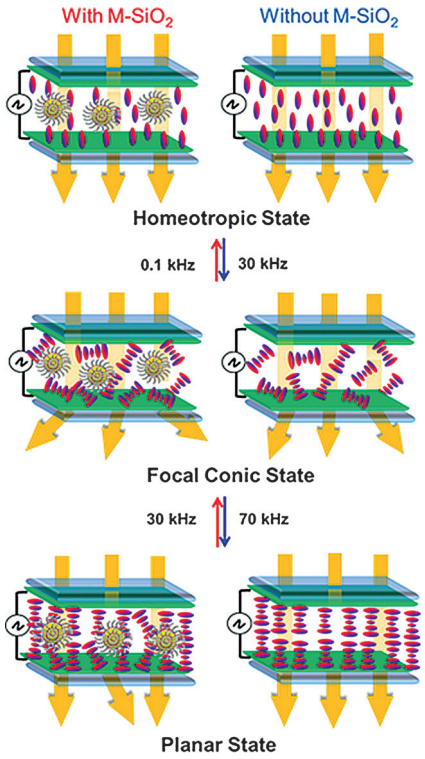

Figure 6. a) Schematic illustration of M-SiO_2-doped DFCLC nanocomposite (left) and pure DFCLC (right) in the LC cell at three different states driven by different frequencies but under constant voltage.

molecules tend to align parallel to the vertical electric field due to the LC exhibiting a positive dielectric anisotropy ($\Delta\varepsilon > 0$) where the homeotropic state is preferred (Figure 6 top). An increase in the frequency induced the cholesteric organization but the helical axes are randomly oriented resulting in the FC state, that is, scattered state (Figure 6 middle). When the frequency is further raised, the helical axes orient parallel to the electric field due to the LC exhibiting a negative dielectric anisotropy ($\Delta\varepsilon < 0$), assembling into the planar configuration (Figure 6 bottom). Doping M-SiO_2 nanoparticles might result in the increase of defect density in the helix configuration and subsequently a stronger light scattering due to the refractive index mismatching among FC multi-domains; other possible explanation of the achievement of higher contrast ratio could be attributed to the dynamic turbulence of the nanoparticles in LC media when subjected to the fields at higher frequencies, where an enhanced scattering is produced by localized variations in the index of refraction at both FC and planar states.

In summary, we have designed and functionalized silica nanoparticles with a covalently attached mesogenic monolayer through a silane coupling agent. The resulting M-SiO_2 nanoparticles were soluble in organic solvents and characterized by ^{1}H NMR spectroscopy, TGA, UV/Vis, TEM, and EDX techniques. The organo-soluble M-SiO_2 nanoparticles were doped into a dual frequency cholesteric LC medium with different concentrations (0.5–3.0 wt%) exhibiting superior dispersion. From the electro-optical measurements, it was found that doping silica nanoparticles was able to greatly improve the contrast ratio of the nanocomposites compared with the pure DFCLC, which might result from the refractive index mismatching among FC multi-domains, and the dynamic turbulence of the nanoparticles in LC cell when subjected to the fields at higher frequencies. The optimal contrast ratio for both FC and planar states was achieved in 2 wt% M-SiO_2 doped DFCLC nanocomposite. Importantly, three stable states, that is, transparent, opaque, and partially transparent, were accomplished by doping M-SiO_2 nanoparticles into the DFCLC under different frequencies at low applied voltage, which indicates that it is possible to make devices with tunable transparency with such functional materials. This work disclosed here to enhance scattering and reversibly control molecular orientation driven by frequency through hybrid nanoparticles offers an impetus in developing dynamic functional architectures and devices such as smart windows. Moreover, the synthetic route demonstrated here could provide an easy access to synthesize diverse surface-functionalized SiO_2 nanoparticles with desired properties, which could improve the properties of other liquid-crystalline systems through nanoparticle–LC synergistic interaction.

Acknowledgements

We thank the support from the AFOSR, AFRL, NIH (through grant number R01EY020641) and the State of Ohio TVSF fund (through grant number TECG201604); the CONACYT Scholarship 211982 (Mexico) to K.G. and China Scholarship Council to Z.Z. are gratefully acknowledged. The TEM data were obtained at the (cryo) TEM facility at the LCI supported by the Ohio Research Scholars Program Research Cluster on Surfaces in Advanced Materials.

Keywords: helical superstructures · liquid crystals · silica nanoparticles · self-organization · frequency dependence · tunable transparency

How to cite: *Angew. Chem. Int. Ed.* **2016**, *55*, 13090–13094
Angew. Chem. **2016**, *128*, 13284–13288

[1] a) *Chirality in Liquid Crystals* (Ed.: H.-S. Kitzerow, C. Bahr), Springer, New York, **2001**; b) Z. Zheng, Y. Li, H. K. Bisoyi, L. Wang, T. J. Bunning, Q. Li, *Nature* **2016**, *531*, 352–356; c) L. Wang, Q. Li, *Adv. Funct. Mater.* **2016**, *26*, 10–28; d) H. K. Bisoyi, Q. Li, *Angew. Chem. Int. Ed.* **2016**, *55*, 2994–3010; *Angew. Chem.* **2016**, *128*, 3046–3063.

 © 2016 Wiley-VCH Verlag GmbH & Co. KGaA, Weinheim

[2] a) M. Xu, D.-K. Yang, *Appl. Phys. Lett.* **1997**, *70*, 720 – 722; b) Y.-C. Hsiao, C.-Y. Tang, W. Lee, *Opt. Express* **2011**, *19*, 9744 – 9749; c) P. Kumar, S.-W. Kang, S. H. Lee, *Opt. Mater. Express* **2012**, *2*, 1121 – 1134; d) J. Ma, L. Shi, D.-K. Yang, *Appl. Phys. Express* **2010**, *3*, 021702; e) K.-T. Cheng, P.-Y. Lee, M. M. Qasim, C.-K. Liu, W.-F. Cheng, T. D. Wilkinson, *ACS Appl. Mater. Interfaces* **2016**, *8*, 10483 – 10493.

[3] a) H. K. Bisoyi, S. Kumar, *Chem. Soc. Rev.* **2011**, *40*, 306 – 319; b) L. Wang, K. G. Gutierrez-Cuevas, H. K. Bisoyi, J. Xiang, G. Gautam, R. S. Zola, S. Kumar, O. D. Lavrentovich, A. Urbas, Q. Li, *Chem. Commun.* **2015**, *51*, 15039 – 15042; c) L. Wang, K. G. Gutierrez-Cuevas, A. Urbas, Q. Li, *Adv. Opt. Mater.* **2016**, *4*, 247 – 251; d) R. Kumar, K. K. Raina, *Liq. Cryst.* **2015**, *42*, 119 – 126.

[4] a) M. Kreuzer, T. Tschudi, *Appl. Phys. Lett.* **1993**, *62*, 1712 – 1714; b) A. Jákli, L. Almásy, S. Borbély, L. Rosta, *Eur. Phys. J. B* **1999**, *10*, 509 – 513; c) N. J. Diorio, Jr., M. R. Fisch, J. W. West, *Liq. Cryst.* **2002**, *29*, 589 – 596.

[5] J. C. Payne, E. L. Thomas, *Adv. Funct. Mater.* **2007**, *17*, 2717 – 2721.

[6] a) W. Li, M. Zhu, X. Ding, B. Li, W. Huang, H. Cao, Z. Yang, H. Yang, *J. Appl. Polym. Sci.* **2009**, *111*, 1449 – 1453; b) P. Kumar, K. K. Raina, *Opt. Mater.* **2012**, *34*, 1878 – 1884; c) C.-J. Hsu, C.-C. Kuo, C.-D. Hsieh, C.-Y. Huang, *Opt. Express* **2014**, *22*, 18513 – 18518.

[7] a) V. Rachet, K. Lahlil, M. Bérard, T. Gacoin, J.-P. Boilot, *J. Am. Chem. Soc.* **2007**, *129*, 9274 – 9275; b) A. Glushchenko, H. Kresse, V. Reshetnyak, Y. Reznikov, O. Yaroshchuk, *Liq. Cryst.* **1997**, *23*, 241 – 246; c) J. D. Busbee, A. T. Juhl, L. V. Natarajan, V. P. Tongdilia, T. J. Bunning, R. A. Vaia, P. V. Braun, *Adv. Mater.* **2009**, *21*, 3659 – 3662.

[8] a) C. Xue, J. Xiang, H. Nemati, H. K. Bisoyi, K. G. Gutierrez-Cuevas, L. Wang, M. Gao, S. Zhou, D.-K. Yang, O. D. Lavrentovich, A. Urbas, Q. Li, *ChemPhysChem* **2015**, *16*, 1852 – 1856; b) W. Lewandowski, M. Wójcik, E. Górecka, *ChemPhysChem* **2014**, *15*, 1283 – 1295.

[9] a) Y. Nakahara, T. Takeuchi, S. Yokoyama, K. Kimura, *Surf. Interface Anal.* **2011**, *43*, 809 – 815; b) A. S. Heintz, M. J. Fink, B. S. Mitchell, *Appl. Organomet. Chem.* **2010**, *24*, 236 – 240.

[10] a) M. V. Gorkunov, M. A. Osipov, *Soft Matter* **2011**, *7*, 4348 – 4356; b) K. G. Gutierrez-Cuevas, L. Wang, C. Xue, G. Singh, S. Kumar, A. Urbas, Q. Li, *Chem. Commun.* **2015**, *51*, 9845 – 9848.

Received: July 15, 2016
Revised: August 9, 2016
Published online: September 16, 2016

 © 2016 Wiley-VCH Verlag GmbH & Co. KGaA, Weinheim